Cell

A Conserved MST-FOXO Signaling Pathway Mediates Oxidative-Stress Responses and Extends Life Span

Maria K. Lehtinen,[1,2,6] Zengqiang Yuan,[1,6] Peter R. Boag,[1,5] Yue Yang,[1,2] Judit Villén,[4] Esther B.E. Becker,[1,3] Sara DiBacco,[1] Núria de la Iglesia,[1] Steven Gygi,[4] T. Keith Blackwell,[1,5] and Azad Bonni[1,2,3,*]
[1] Department of Pathology
[2] Program in Neuroscience
[3] Program in Biomedical and Biological Sciences
[4] Department of Cell Biology
Harvard Medical School, Boston, MA 02115, USA
[5] Section on Developmental and Stem Cell Biology, Joslin Diabetes Center, One Joslin Place, Boston, MA 02215, USA
[6] These authors contributed equally to this work.
*Contact: azad_bonni@hms.harvard.edu
DOI 10.1016/j.cell.2006.03.046

SUMMARY

Oxidative stress influences cell survival and homeostasis, but the mechanisms underlying the biological effects of oxidative stress remain to be elucidated. Here, we demonstrate that the protein kinase MST1 mediates oxidative-stress-induced cell death in primary mammalian neurons by directly activating the FOXO transcription factors. MST1 phosphorylates FOXO proteins at a conserved site within the forkhead domain that disrupts their interaction with 14-3-3 proteins, promotes FOXO nuclear translocation, and thereby induces cell death in neurons. We also extend the MST-FOXO signaling link to nematodes. Knockdown of the *C. elegans* MST1 ortholog CST-1 shortens life span and accelerates tissue aging, while overexpression of *cst-1* promotes life span and delays aging. The *cst-1*-induced life-span extension occurs in a *daf-16*-dependent manner. The identification of the FOXO transcription factors as major and evolutionarily conserved targets of MST1 suggests that MST kinases play important roles in diverse biological processes including cellular responses to oxidative stress and longevity.

INTRODUCTION

Oxidative stress impacts diverse biological processes, including cell survival and aging as well as the pathogenesis of many diseases ranging from diabetes to neurodegenerative disorders of the brain (Beckman and Ames, 1998; Chong et al., 2005). Oxidative stress is thought to trigger alterations of gene expression that culminate in either programmed cell death or cell recovery (Chong et al., 2005; Finkel, 2000). However, the intracellular mechanisms by which oxidative-stress signals are relayed to the nucleus remain incompletely understood.

Protein kinases play a central role in signaling to the nucleus in response to extrinsic cues including growth factors (Karin and Hunter, 1995). Likewise, protein kinases are thought to regulate cellular responses to oxidative stress (Finkel, 2000). The protein kinase Sterile 20 (Ste20) was recently discovered to mediate hydrogen-peroxide-induced cell death in *S. cerevisiae* (Ahn et al., 2005). The mammalian Ste20-like kinases (MSTs), of which MST1 and MST2 share the highest degree of homology, and the *Drosophila* ortholog Hippo have important functions in apoptotic cell death (Cheung et al., 2003; Graves et al., 1998; Harvey et al., 2003; O'Neill et al., 2004; Wu et al., 2003). Together, these observations raise the question of whether MST plays a role in oxidative-stress responses in higher eukaryotes.

The FOXO transcription factors induce apoptotic or adaptive responses in mammalian cells upon exposure to oxidative stress (Brunet et al., 2004; Kops et al., 2002). At an organismal level, studies in *C. elegans* have not implicated the FOXO ortholog DAF-16 in cell death but have established a major role for DAF-16 in promoting longevity (reviewed in Kenyon, 2005). The *Drosophila* protein dFOXO also promotes life span, suggesting that FOXO function in longevity is conserved across evolution (Giannakou et al., 2004; Hwangbo et al., 2004).

Regulation of FOXO proteins has been extensively characterized in the context of growth-factor signaling (reviewed in Burgering and Kops, 2002; Van Der Heide et al., 2004). The insulin-like growth factor (IGF) induced phosphoinositide-3 kinase (PI3K) Akt kinase cascade inhibits the activity of FOXO proteins (Brunet et al., 2001).

Akt directly phosphorylates FOXO proteins at distinct sites and thereby stimulates their association with 14-3-3 proteins and sequestration in the cytoplasm (Van Der Heide et al., 2004). Regulation of FOXO proteins by the insulin-PI3K-Akt signaling pathway is conserved from *C. elegans* to mammals (Kenyon, 2005; Van Der Heide et al., 2004). Thus, while deficiency of the insulin-regulated PI3K-Akt signaling pathway leads to the activation of DAF-16 and thereby promotes life-span extension in nematodes, inhibition of this signaling pathway and consequent activation of FOXO transcription factors triggers cell death in mammalian cells (Brunet et al., 2001; Kenyon, 2005).

In this study, we identify the FOXO transcription factors as evolutionarily conserved key targets of the MST family of kinases. We find that MST1 phosphorylates the FOXO transcription factors at a site that is conserved within the forkhead domain of these proteins from mammals to *C. elegans*. In mammalian neurons, oxidative stress activates MST1, which in turn phosphorylates FOXO3 at serine 207. The MST1-induced phosphorylation of FOXO3 disrupts FOXO3's interaction with 14-3-3 proteins, promotes FOXO3 translocation to the nucleus, and thereby induces neuronal cell death. We also find that MST-FOXO signaling operates in nematodes. MST1 can phosphorylate DAF-16 at serine 196, which corresponds to FOXO3 serine 207. Knockdown of the *C. elegans* MST1 ortholog CST-1 accelerates aging and reduces life span. In contrast, overexpression of *cst-1* promotes life span and delays tissue aging. Importantly, the *cst-1*-induced life-span extension is dependent on *daf-16*, supporting the conclusion that CST-DAF-16 signaling promotes longevity in *C. elegans*. Taken together, our findings demonstrate an intimate and evolutionarily conserved signaling link between MST1 and FOXO transcription factors that regulates responses to oxidative stress in mammalian cells and longevity in nematodes.

RESULTS

MST1 Mediates Oxidative-Stress-Induced Cell Death via FOXO Transcription Factors

We characterized a potential role of MST1 in oxidative-stress responses in mammalian cells. Primary granule neurons of the rat cerebellum provide a robust system for the study of cell death, including upon exposure to oxidative stress (Becker and Bonni, 2004). We found that exposure of granule neurons to hydrogen peroxide stimulated the increased autophosphorylation of MST1/2 (Figure 1A), suggesting that the MST family of kinases is activated in neurons in response to oxidative stress.

To determine the importance of oxidative-stress-induced endogenous MST1 in neurons, we employed a plasmid-based method of RNA interference (RNAi). Expression of MST1 hairpin RNAs (hpRNAs) reduced effectively the expression of MST1 in granule neurons (Figure 1B). We next transfected primary neurons with the MST1 RNAi or control U6 plasmid, and 3 days after transfection, neurons were left untreated or were treated with hydrogen peroxide for 24 hr. Exposure of control U6-transfected neurons to hydrogen peroxide robustly induced cell death. However, MST1 knockdown neurons were protected from hydrogen-peroxide-induced cell death (Figure 1C). These data suggest that MST1 is required for oxidative-stress-induced neuronal cell death.

To demonstrate the specificity the MST1 RNAi phenotype in neurons, we performed a rescue experiment. We generated a "rescue" form of MST1 (MST1R) that is resistant to MST1 RNAi (Figure 1D). MST1R, but not MST1, significantly reduced the ability of MST1 knockdown to protect neurons from hydrogen-peroxide-induced cell death (Figure 1E). Thus, MST1 RNAi inhibits hydrogen-peroxide-induced cell death via specific knockdown of MST1 rather than off-target effects of RNAi.

We next investigated the mechanism by which MST1 promotes neuronal cell death. In *S. cerevisiae*, hydrogen peroxide triggers the translocation of full-length Ste20 to the nucleus, where Ste20 phosphorylates histone H2B at serine 10 (Ahn et al., 2005). In mammalian cells, the cytotoxic agent etoposide induces the cleavage of an N-terminal fragment of MST1 that localizes to the nucleus and phosphorylates histone H2B at serine 14 (Cheung et al., 2003). We were unable to demonstrate that hydrogen peroxide induces the nuclear translocation of MST1 or the phosphorylation of histone H2B at serine 14 in mammalian cells and neurons (data not shown). These observations raised the possibility that MST1 might couple oxidative-stress signals to the nucleus via proteins that undergo nucleocytoplasmic shuttling.

The FOXO proteins transit between the cytoplasm and nucleus and mediate responses to oxidative stress including neuronal death (Brunet et al., 2004; Essers et al., 2004). We therefore determined whether MST1 might mediate oxidative-stress-induced cell death in neurons via FOXO proteins. Induction of FOXO RNAi, but not of the unrelated protein Cdk2, protected neurons from hydrogen-peroxide-induced cell death (Figure 1F), suggesting a requirement for FOXO-family proteins in oxidative-stress-induced neuronal cell death. In other experiments, expression of exogenous MST1 in neurons induced cell death, but knockdown of FOXO proteins suppressed MST1-induced cell death (Figure 1G). Together, these results suggest that MST1 mediates oxidative-stress-induced cell death in a FOXO-dependent manner.

MST1 Phosphorylates FOXO3 at a Conserved Site In Vitro and In Vivo

Since MST1 is a protein kinase, we next tested whether MST1 might phosphorylate FOXO proteins. We found that MST1, but not a kinase-dead MST1 in which the ATP binding site was mutated (MST1 K59R), phosphorylated FOXO3 in vitro (Figure 2A). Upon expression in 293T cells, MST1 and FOXO3 formed a physical complex (Figure 2B). We also found that endogenous MST1, but not the protein kinase MLK3, associated with endogenous FOXO3 in cells (Figure 2C). The interaction of MST1 and FOXO3 supported the possibility that FOXO3 might be a substrate of MST1.

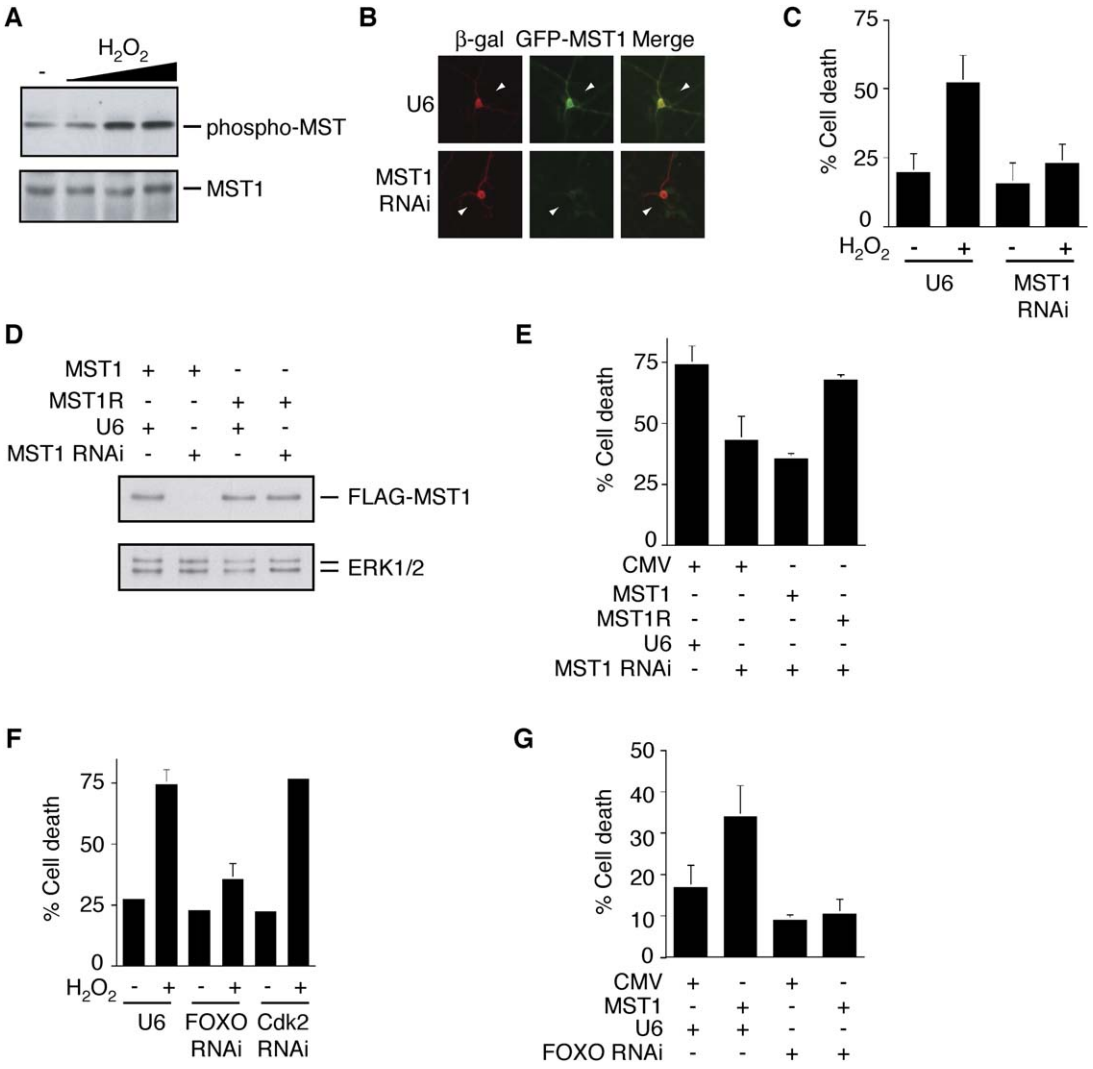

Figure 1. MST1 Mediates Oxidative-Stress-Induced Neuronal Cell Death via FOXO Transcription Factors

(A) Lysates of granule neurons treated with increasing concentrations of H_2O_2 (0–100 μM) for 30 min were immunoblotted with phospho-MST1/2 and MST1 antibodies.

(B) Immunocytochemical analysis of granule neurons transfected with GFP-MST1 and β-galactosidase expression plasmids together with the MST1 RNAi or control U6 plasmid. MST1 RNAi reduced GFP-MST1 expression in 91.3% of transfected cells (t test; $p < 0.0001$, $n = 3$).

(C) Granule neurons were transfected with the MST1 RNAi or control U6 plasmid together with the β-galactosidase expression plasmid. Percent cell death in transfected β-galactosidase-positive neurons is represented as mean ± SEM. Cell death was significantly increased upon H_2O_2 treatment in U6-transfected neurons but not in MST1 knockdown neurons (ANOVA; $p < 0.05$, $n = 4$). In these and other survival experiments, H_2O_2 treatment similarly induced cell death in untransfected neurons in cultures transfected with different test plasmids (data not shown).

(D) Lysates of 293T cells transfected with an expression vector encoding FLAG-MST1 or FLAG-MST1R together with the MST1 RNAi or control U6 plasmid were immunoblotted with the FLAG and ERK1/2 antibodies.

(E) Neurons transfected with the FLAG-MST1 or FLAG-MST1R expression plasmid and the β-galactosidase expression vector together with the MST1 RNAi plasmid were treated with H_2O_2 and analyzed as in (C). MST1R blocked the ability of MST1 RNAi to protect neurons from H_2O_2-induced death (ANOVA; $p < 0.001$, $n = 3$).

(F) Neurons transfected with the FOXO RNAi, Cdk2 RNAi, or control U6 plasmid together with the β-galactosidase expression vector were left untreated or treated with H_2O_2 and analyzed as in (C). FOXO knockdown protected neurons from H_2O_2-induced death (ANOVA; $p < 0.0001$, $n = 3$).

(G) Neurons were transfected with the FLAG-MST1 and β-galactosidase expression vectors together with the FOXO RNAi or control U6 plasmid. After 72 hr, cultures were analyzed as in (C). FOXO knockdown blocked MST1-induced neuronal death (ANOVA; $p < 0.05$, $n = 3$).

We delineated the region within FOXO3 that associates with MST1 in GST pull-down assays using recombinant GST fusion proteins encoding five nonoverlapping FOXO3 regions (peptides P1–P5). MST1 coprecipitated only with peptide P2 (amino acids 154–259), which contains the forkhead domain (Figure 2D). MST1 robustly

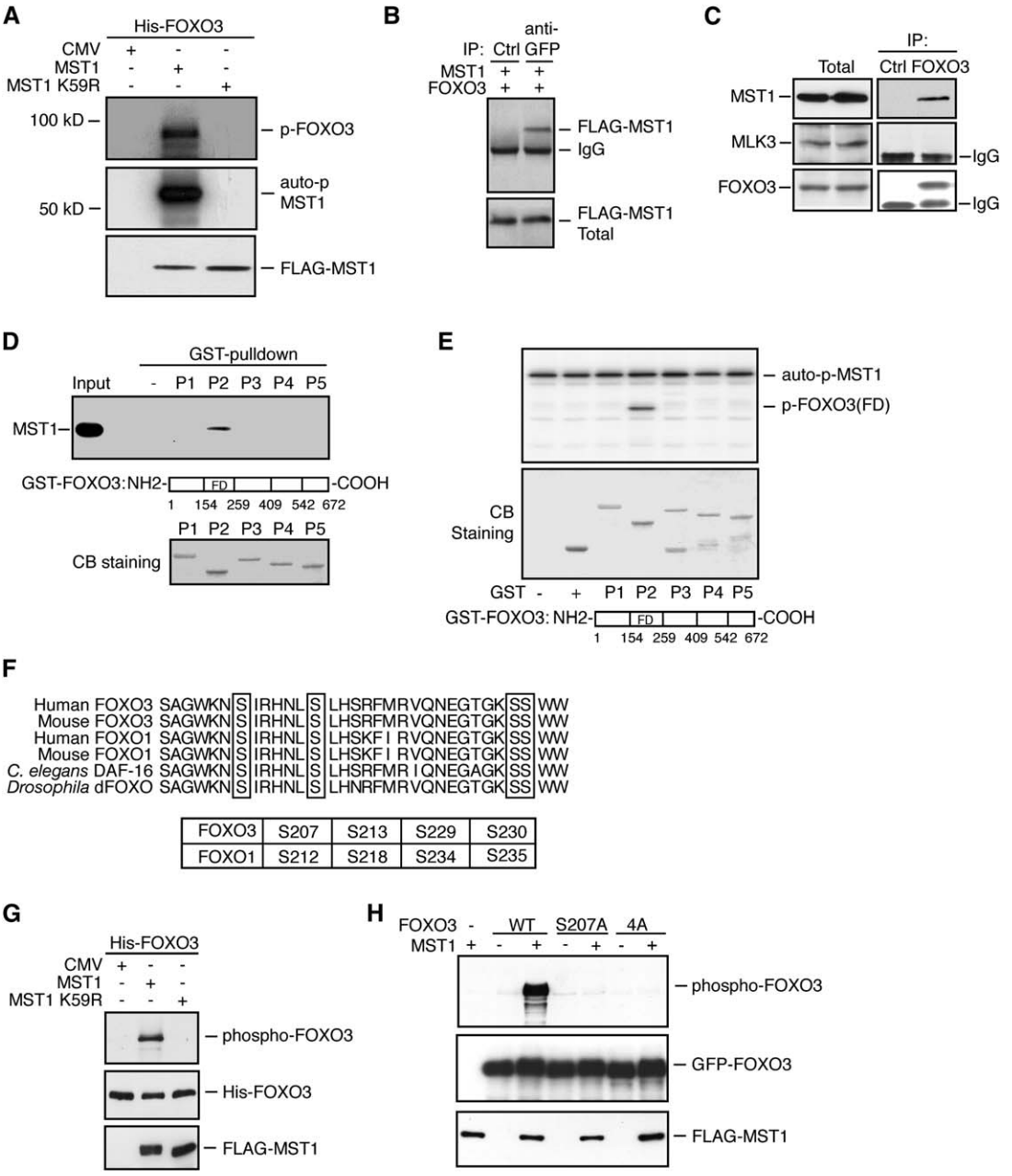

Figure 2. MST1 Interacts with and Phosphorylates FOXO3 within the Forkhead Domain

(A) Lysates of 293T cells transfected with an expression vector encoding FLAG-MST1, kinase-dead FLAG-MST1 K59R, or the control plasmid were immunoprecipitated with the FLAG antibody and subjected to an in vitro kinase assay using full-length His-FOXO3 as substrate in the presence of [^{32}P]ATP. Auto-p denotes autophosphorylated MST1. Lower panel shows the expression of MST1 and MST1 K59R by immunoblotting.

(B) Lysates of 293T cells transfected with the GFP-FOXO3 and FLAG-MST1 expression plasmids were immunoprecipitated with the GFP or control HA (Ctrl) antibody followed by immunoblotting with the FLAG antibody.

(C) Lysates of 293T cells were immunoprecipitated with the control HA (Ctrl) or a rabbit antibody to FOXO3 followed by immunoblotting with an antibody to MST1, MLK3, or FOXO3.

(D) GST pull-down assays of FLAG-MST1 with recombinant GST or GST fused with fragments of FOXO3 (P1–P5). Precipitated proteins were immunoblotted with the FLAG antibody. Lower panel is Coomassie blue (CB) staining of GST-FOXO3 peptides.

(E) In vitro kinase assays using FLAG-MST1 with no substrate, recombinant GST, or recombinant GST-FOXO3 peptides were done as in (A).

(F) Alignment of sequences in the forkhead domain of mammalian FOXO3 and FOXO1, *C. elegans* DAF-16, and *Drosophila* dFOXO.

(G) Lysates of 293T cells transfected with FLAG-MST1, FLAG-MST1 K59R, or the control vector were immunoprecipitated with the FLAG antibody and subjected to an in vitro kinase assay using recombinant His-FOXO3 as substrate. Phosphorylation reactions were analyzed by immunoblotting with the phospho-FOXO, His, or FLAG antibody.

phosphorylated the P2 fragment but not the other FOXO3 fragments in vitro (Figure 2E). These results suggest that MST1 specifically interacts with and phosphorylates the forkhead domain of FOXO3.

By tandem mass spectrometry analysis (MS/MS) aided by data-dependent MS/MS/MS (MS^3), we identified four serine residues (serines 207, 213, 229 or 230, and 241) that were phosphorylated by MST1 in the forkhead domain of FOXO3 (see Table S1 in the Supplemental Data available with this article online). These serines are highly conserved among FOXO family members and across species including vertebrates, *C. elegans*, and *Drosophila* (Figure 2F). MST1 phosphorylated the conserved sites in the FOXO1 forkhead domain in vitro but failed to phosphorylate FOXO1 forkhead-domain mutants in which serine 212 (corresponding to serine 207 in FOXO3) was replaced with alanine (data not shown). Together, these experiments demonstrate that MST1 phosphorylates the forkhead domain of FOXO transcription factors on distinct sites in vitro and suggest that one of these sites (serine 207 in FOXO3) represents the principal MST1 phosphorylation site.

We raised a rabbit antiserum to specifically recognize FOXO proteins when phosphorylated at the conserved MST1 site. The phospho-FOXO antibody recognized recombinant FOXO3 that was phosphorylated by MST1 in vitro but did not recognize recombinant FOXO3 that was unphosphorylated or that was incubated with the kinase-dead MST1 K59R (Figure 2G). The phospho-FOXO antibody also specifically recognized the forkhead domain of FOXO3 (FOXO3-FD) that was phosphorylated by purified recombinant MST1 in vitro (Figure S1). We also found that the phospho-FOXO antibody recognized GFP-FOXO3 but not the serine 207 mutants of GFP-FOXO3 that were coexpressed with MST1 in cells (Figure 2H). Taken together, our results show that MST1 induces the phosphorylation of FOXO3 at the conserved site serine 207 within the forkhead domain both in vitro and in vivo.

We next determined whether oxidative stress induces the MST1-mediated FOXO phosphorylation in cells and neurons. Hydrogen peroxide induced the endogenous FOXO3 phosphorylation at serine 207 in both 293T cells (Figure S2) and primary neurons (Figures 3A and 3B). In the immunocytochemical analyses in neurons, the phospho-FOXO signal was specifically competed with the phosphorylated but not unphosphorylated FOXO peptide (Figure 3B). Hydrogen peroxide also stimulated the interaction of endogenous MST1 and FOXO3 in cells and primary neurons (Figure 3C), supporting the possibility that FOXO3 might be a key substrate of MST1 in response to oxidative stress. Knockdown of MST1 in cells impaired hydrogen-peroxide-induced phosphorylation of endogenous FOXO3 at serine 207 (Figure 3D). In neurons, knockdown of MST1 or MST2, but not of the protein kinase Cdk2, reduced the ability of hydrogen peroxide to effectively induce the FOXO3 phosphorylation (Figure 3E). Taken together, these results support the conclusion that the MST family of kinases phosphorylates FOXO3 at the conserved forkhead-domain site serine 207 in cells and primary neurons upon oxidative stress.

MST1 Phosphorylation of FOXO3 Disrupts its Interaction with 14-3-3 Proteins and Promotes FOXO3 Translocation to the Nucleus

The hydrogen-peroxide-induced MST1 phosphorylation of FOXO3 at serine 207 led us to determine the consequences of this phosphorylation event. Since MST1 interacts with FOXO3 in the cytoplasmic compartment of the cells (data not shown), we next asked whether MST1-induced phosphorylation of FOXO3 might regulate FOXO3's sequestration by 14-3-3 proteins in the cytoplasm. We expressed GFP-FOXO3 together with MST1 or the kinase-dead MST1 K59R in 293T cells. Expression of MST1, but not MST1 K59R, reduced the amount of 14-3-3 that interacted with GFP-FOXO3 (Figure 4A). These results suggest that MST1 disrupts the association of FOXO3 with 14-3-3 proteins.

We next determined the role of the MST1-induced FOXO3 phosphorylation at serine 207 in the inhibition of FOXO3's interaction with 14-3-3 proteins. While expression of MST1 robustly disrupted the interaction of 14-3-3 proteins with GFP-FOXO3, MST1 failed to inhibit the interaction of 14-3-3 with GFP-FOXO3 mutants in which serine 207 was replaced with alanine (Figure 4B). MST1 failed to inhibit the phosphorylation of FOXO3 at serine 253 (data not shown), an Akt-induced phosphorylation event that promotes FOXO3's interaction with 14-3-3 proteins (Brunet et al., 2001). These results suggest that MST1-induced phosphorylation of FOXO3 at serine 207 triggers the dissociation of FOXO3 from 14-3-3 proteins.

We next characterized the role of endogenous MST in the control of FOXO3's interaction with 14-3-3 proteins in response to oxidative stress. Exposure of 293T cells to hydrogen peroxide led to a significant reduction in the association of 14-3-3 proteins with endogenous FOXO3 or exogenously expressed GFP-FOXO3 (Figures 4C and 4D). Although induction of MST1 RNAi alone had little effect (data not shown), knockdown of both MST1 and MST2 together blocked the ability of hydrogen peroxide to inhibit the interaction of 14-3-3 with GFP-FOXO3 in 293T cells (Figure 4D). Thus, endogenous MST mediates the ability of oxidative stress to trigger the dissociation of FOXO3 and 14-3-3 proteins in cells.

Since 14-3-3 proteins sequester FOXO transcription factors in the cytoplasm (Van Der Heide et al., 2004), we reasoned that the MST-induced disruption of FOXO3-14-3-3 binding might influence the localization of FOXO3. To measure the effect of MST1 on the subcellular localization of FOXO3, we employed CCL39 cells, which are optimal for localization studies of FOXO3. MST1, but not MST1

(H) Lysates of 293T cells transfected with the FLAG-MST1 expression vector or the control plasmid together with expression plasmids encoding GFP-FOXO3 or GFP-FOXO3 mutants were subjected to immunoblotting with the phospho-FOXO, GFP, or FLAG antibody.

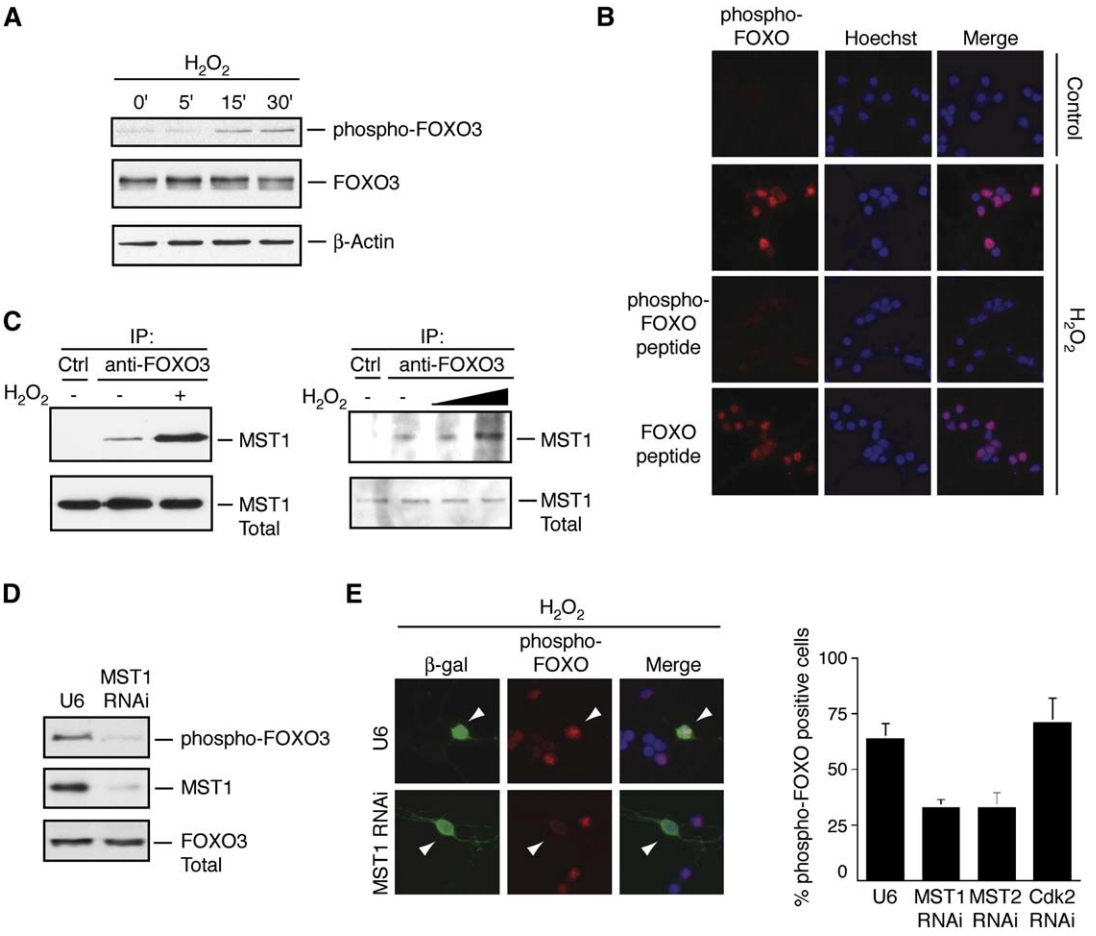

Figure 3. MST1 Mediates Oxidative-Stress-Induced Phosphorylation of FOXO3 at Serine 207

(A) Lysates of granule neurons left untreated or treated with H_2O_2 for indicated times were subjected to immunoblotting with the phospho-FOXO, FOXO3, or β-actin antibody.

(B) Neurons left untreated or treated with H_2O_2 for 1 hr were subjected to immunocytochemical analysis with the phospho-FOXO antibody. H_2O_2-induced endogenous FOXO3 phosphorylation (sustained at 1 hr, declining at 3 hr, and very low at 24 hr [data not shown]) preceded cell death.

(C) Lysates of 293T cells (left panels) or primary neurons (right panels) left untreated or treated with H_2O_2 were immunoprecipitated with the FOXO3 or control HA (Ctrl) antibody followed by immunoblotting with the MST1 antibody.

(D) Lysates of 293T cells transfected with the MST1 RNAi or control U6 plasmid and then treated with H_2O_2 for 1 hr were immunoblotted with the phospho-FOXO, MST1, or FOXO3 antibody.

(E) Left panels: Immunocytochemical analysis of granule neurons that were transfected with the MST1, MST2, or Cdk2 RNAi plasmid or the control U6 plasmid together with the β-galactosidase expression vector and then treated with H_2O_2 for 1 hr. Arrowheads indicate transfected neurons that were analyzed for phospho-FOXO staining. Right panels: MST1 and MST2 knockdown inhibited H_2O_2-induced FOXO phosphorylation as compared to control (ANOVA; $p < 0.01$, $n = 3$). Data are represented as mean ± SEM.

K59R, stimulated the accumulation of GFP-FOXO3 in the nucleus of these cells (Figure S3). However, MST1 failed to induce the nuclear accumulation of the GFP-FOXO3 mutants in which serine 207 was replaced with alanine (Figure 4E). In neurons, hydrogen peroxide induced the translocation of GFP-FOXO3 but not of the GFP-FOXO3 S207A mutant (Figure 4F). These results suggest that the phosphorylation of FOXO3 at serine 207 mediates hydrogen-peroxide-induced FOXO3 translocation to the nucleus. In control experiments, mutation of serine 207 had little effect on direct binding of FOXO3 to promoter of the FOXO3 target gene *bim* (Figure S4 and data not shown).

MST-FOXO Signaling Mediates Oxidative-Stress-Induced Transcription and Neuronal Death

The identification of a signaling link between MST1 and FOXO3 that leads to the nuclear translocation of FOXO3 raised the possibility that the MST-FOXO pathway might couple oxidative-stress signals to gene transcription and cell death. The FOXO3 target gene *bim* encodes a BH3-only protein that directly activates the cell death machinery (Gilley et al., 2003). Hydrogen peroxide induced the expression of BIM protein in cells and neurons (Figures 5A and 5B). MST1 knockdown reduced the hydrogen-peroxide-induced expression of BIM (Figure 5B). In

addition, MST1 and FOXO knockdown both significantly reduced BIM promoter-mediated transcription in hydrogen-peroxide-treated granule neurons (Figure 5C).

We next determined the significance of the MST1-induced FOXO3 phosphorylation in oxidative-stress-induced neuronal cell death. Expression of an RNAi-resistant form of FOXO3 (FOXO3R), but not FOXO3 that is encoded by wild-type cDNA, reversed the ability of FOXO RNAi to protect neurons from hydrogen-peroxide-induced cell death (Figures 5D and 5E). In contrast to FOXO3R, FOXO3R mutants in which serine 207 was replaced with alanine (FOXO3R S207A or FOXO3R 4A) failed to mediate neuronal cell death in the background of FOXO RNAi (Figure 5E). In control experiments, mutation of serine 207 had no effect on the amount of FOXO3R expression (Figure 5E). These results indicate that phosphorylation of FOXO3 at serine 207 is required for the ability of FOXO3 to mediate hydrogen-peroxide-induced neuronal cell death.

Taken together, our findings suggest that exposure of primary mammalian neurons to acute oxidative stress stimulates the activation of MST1 and its association with FOXO3, leading to the phosphorylation of FOXO3 at serine 207. These MST1-dependent events, which occur with rapid kinetics, in turn induce the dissociation of FOXO3 from 14-3-3 proteins and FOXO3 translocation to the nucleus, culminating in neuronal cell death.

The MST-FOXO Signaling Pathway Promotes Longevity in *C. elegans*

The elucidation of the MST-FOXO signaling pathway in mammalian cells led us next to determine whether this signaling connection is conserved across species. The *C. elegans* model system has provided important insights into the functions and regulation of FOXO proteins (reviewed in Kenyon, 2005). The FOXO ortholog DAF-16 has not been implicated in the regulation of cell death, but DAF-16 is a central positive regulator of organismal longevity (Kenyon, 2005). DAF-16 function is inhibited by the *C. elegans* insulin/IGF1 receptor ortholog DAF-2 (Kenyon, 2005). The entire PI3K-Akt-FOXO signaling cascade is conserved in nematodes and mammals (Kenyon, 2005; Van Der Heide et al., 2004). Therefore, while inhibition of PI3K-Akt signaling triggers FOXO-dependent cell death in mammalian cells (Brunet et al., 2001; Van Der Heide et al., 2004), loss-of-function mutations in components of the DAF-2 signaling pathway, including *daf-2*, *age-1*, and *akt*, extend life span (Kenyon, 2005). Importantly, extension of life span by mutations of DAF-2 and other components of the DAF-2 pathway occurs in a DAF-16-dependent manner (Kenyon, 2005).

Since MST1-induced phosphorylation of FOXO3 activates its function in mammalian cells, MST orthologs in *C. elegans* would be predicted to promote DAF-16's ability to extend life span. To test this hypothesis, we first determined whether MST1 can phosphorylate DAF-16 at serine 196, which corresponds to serine 207 in FOXO3 (Figure 2F). MST1 robustly phosphorylated DAF-16 at the conserved forkhead site serine 196 in vitro and in cells (Figures 6A and 6B). These results are consistent with the possibility that a nematode ortholog of MST1 might promote DAF-16 function in *C. elegans* and thus extend life span.

C. elegans contains two closely related genes that appear to represent orthologs of MST, *cst-1* and *cst-2* (*C. elegans Ste*20-like kinases 1 and 2) (Figures S5A and S5B). Transgenic nematodes that express GFP under the predicted *cst-1* promoter (*Pcst1::gfp*) were generated. In five independent transgenic lines, *Pcst1::gfp* was widely expressed in epidermal cells and was accompanied by intense staining in cells in the tail, vulva, and sensory neurons in the head and weaker expression in the dorsal pharyngeal bulb (Figure 6C).

To assess the function of the CST kinases in aging in *C. elegans*, we induced *cst-1* RNAi by feeding in adult *C. elegans*. Reduction of *cst-1* expression was confirmed by RT-PCR (Figure 6D). Based on the high degree of homology of *cst-1* and *cst-2*, the dsRNA encoded by the *cst-1* RNAi construct is expected to target products of both *cst* genes (Figure S5B); therefore, the effect of the RNAi construct is referred to as CST knockdown. CST knockdown by feeding RNAi had no obvious effects on nematode development (data not shown), but it significantly shortened life span (Figure 6D and Table S2).

Reduction of life span upon gene knockdown may not reflect a specific effect on longevity. Therefore, to determine whether CST specifically regulates life span, we asked whether increasing the expression of *cst-1* in *C. elegans* increases life span. We generated *C. elegans* carrying additional copies of the genomic locus of the *cst-1* gene. Increasing expression of the *cst-1* gene in *C. elegans* significantly increased life span, including the mean and 75th percentile life span (*Ex1050*) (Table S2 and Figure 7A). We also found an increase in maximal life span upon *cst-1* overexpression (experiment 1: 32.3 ± 0.7 days compared to N2 nematodes, 27.3 ± 1.5 days; experiment 2: 31.5 ± 0.5 days compared to N2, 29.3 ± 0.9 days; experiment 3: 24.0 ± 1.0 days compared to N2, 21.5 ± 0.5 days; experiment 4: 28.0 ± 0.6 days compared to N2, 25.0 ± 0.6 days; experiment 5: 25.7 ± 0.9 days compared to N2, 26.0 ± 0.0 days; experiment 6: 25.5 ± 0.5 days compared to N2, 22.5 ± 0.5 days; total number of animals observed/total initial number examined: *Ex1050* = 479/493; N2 = 454/513). Thus, in five out of six experiments, maximal life span was significantly increased upon *cst-1* overexpression as compared to N2 nematodes (t test, $p < 0.05$ in each of the five experiments). These results suggest that CST-1 promotes life span throughout the life of nematodes. Expression of the marker *rol-6* for identification of transgenic nematodes alone (*Ex1060*) did not alter life span (Table S2). Together, these findings suggest that CST-1 extends life span.

We also carried out detailed analyses of age-associated physiological and pathological parameters after CST knockdown or overexpression. CST knockdown led to reduced body movement and pharyngeal pumping at an earlier age than N2 nematodes (Figures 6E and 6F) (Huang

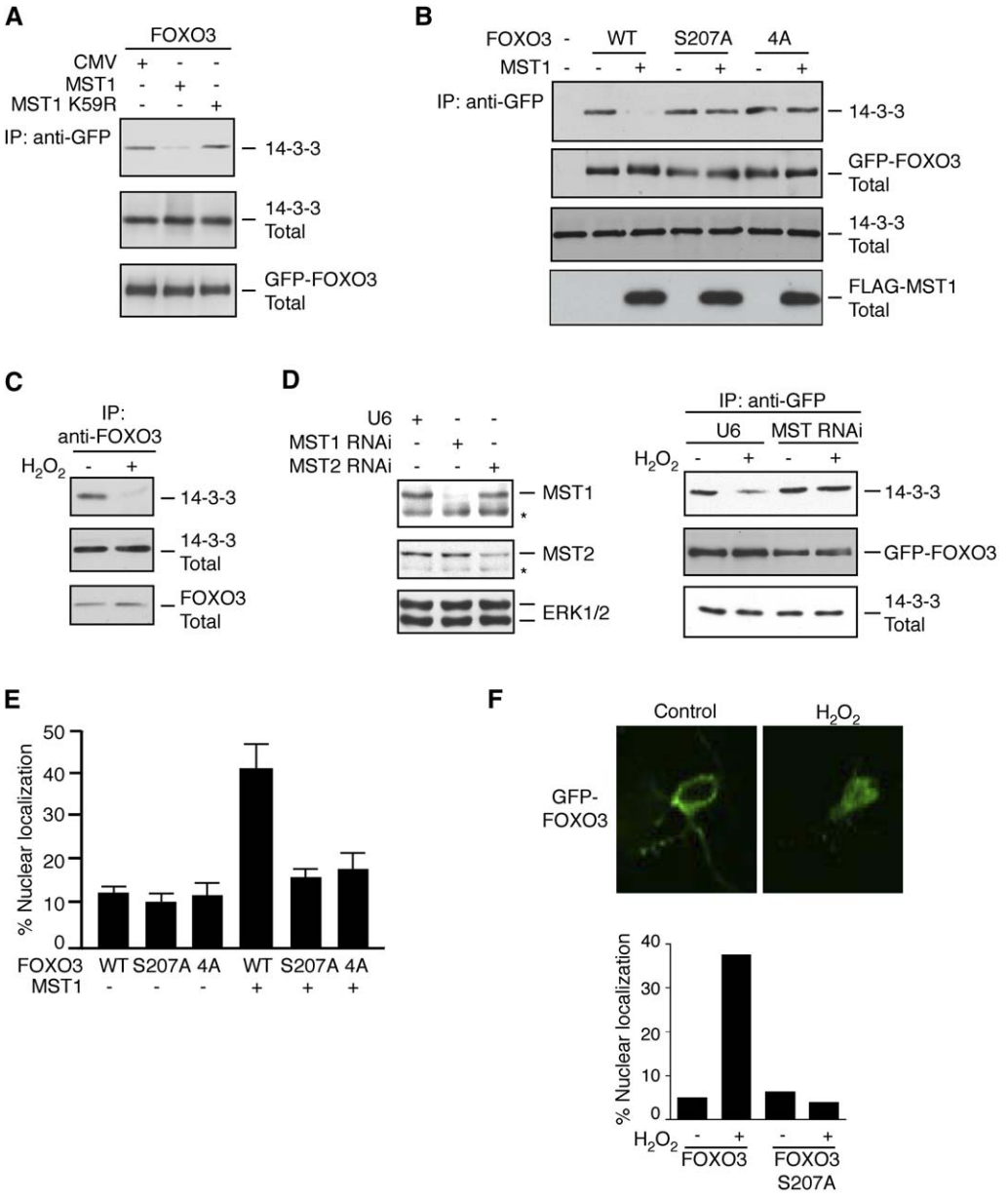

Figure 4. MST1 Phosphorylation of FOXO3 at Serine 207 Disrupts Its Interaction with 14-3-3 Proteins and Promotes FOXO3 Translocation to the Nucleus

(A) Lysates of 293T cells transfected with the GFP-FOXO3 expression plasmid together with an expression vector encoding FLAG-MST1, FLAG-MST1 K59R, or the control vector were immunoprecipitated with the GFP antibody followed by immunoblotting with an antibody against 14-3-3β.

(B) Lysates of 293T cells transfected with expression plasmids encoding wild-type or mutant GFP-FOXO3 together with the FLAG-MST1 expression plasmid or its control vector were immunoprecipitated with the GFP antibody and immunoblotted with the 14-3-3β antibody.

(C) Lysates of 293T cells left untreated or treated with H_2O_2 for 1 hr were immunoprecipitated with the FOXO3 antibody followed by immunoblotting with the 14-3-3β antibody.

(D) Left panels: Lysates of 293T cells transfected with the MST1 and MST2 RNAi plasmids or the control U6 plasmid were immunoblotted with the MST1, MST2, or ERK1/2 antibodies. Asterisks indicate nonspecific bands. Right panels: Lysates of 293T cells transfected with both the MST1 and MST2 RNAi plasmids or the control U6 plasmid together with the GFP-FOXO3 expression plasmid and then left untreated or treated with H_2O_2 were subjected to immunoprecipitation analysis as in (A).

(E) CCL39 cells transfected with expression plasmids encoding wild-type GFP-FOXO3 or its mutants together with the FLAG-MST1 expression plasmid or its control vector were subjected to immunocytochemical analysis with the GFP antibody and the DNA dye bisbenzimide (Hoechst 33258). MST1 induced nuclear localization of wild-type GFP-FOXO3 (ANOVA; $p < 0.01$, $n = 3$) but not the GFP-FOXO3 mutants. A minimum of 200 cells were counted per condition. Data are represented as mean ± SEM.

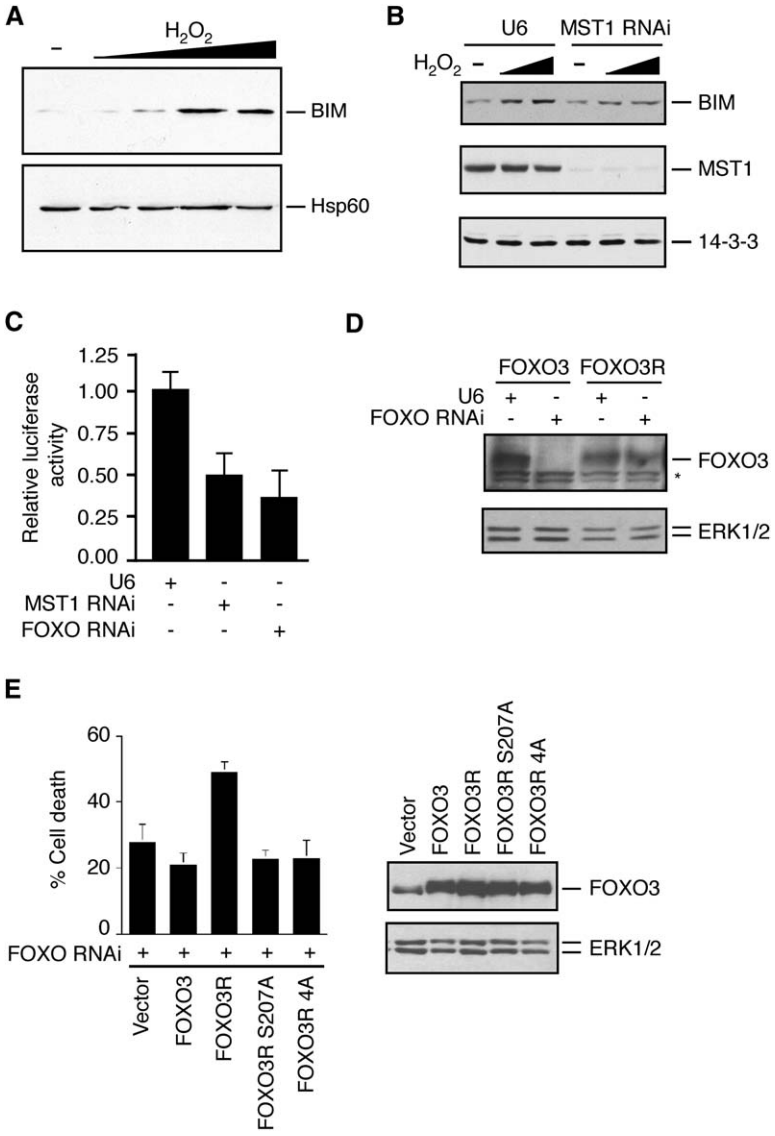

Figure 5. MST-FOXO Signaling Mediates Oxidative-Stress-Induced Neuronal Death

(A) Lysates of neurons treated with increasing concentrations of H_2O_2 (0–100 μM) for 18 hr were immunoblotted with antibodies to BIM and Hsp60.

(B) Lysates of 293T cells transfected with the MST1 RNAi or control U6 plasmid and then treated with increasing concentrations of H_2O_2 (0–50 μM) for 12 hr were subjected to immunoblotting with the BIM, MST1, or 14-3-3β antibody.

(C) Granule neurons were transfected with the MST1 or FOXO RNAi plasmid or control U6 plasmid together with the BIM-luciferase reporter gene and the tk-renilla reporter, the latter to serve as an internal control for transfection efficiency. After 72 hr, cells were treated with H_2O_2 for 12 hr and subjected to luciferase assays. Shown are mean ± SEM of normalized firefly/renilla luciferase values relative to the control U6-transfected neurons. MST1 and FOXO knockdown significantly reduced H_2O_2-induced BIM-luciferase reporter-gene expression (ANOVA; $p < 0.01$, $n = 3$).

(D) Lysates of 293T cells transfected with the FOXO RNAi or control U6 plasmid and a GFP-FOXO3 or GFP-FOXO3R expression vector were immunoblotted with the GFP or ERK1/2 antibodies. Asterisk denotes nonspecific signal. Expression of FOXO hpRNAs induced knockdown of FOXO3 but not FOXO3R.

(E) Left panel: Neurons transfected with the FOXO RNAi plasmid together with expression vectors encoding FOXO3, FOXO3R, FOXO3R S207A, FOXO3R 4A, or their control vector and β-galactosidase were treated with H_2O_2 and analyzed as in Figure 1C. FOXO3R, but not mutants of FOXO3R in which serine 207 was replaced with alanine, blocked the ability of FOXO knockdown to protect neurons from H_2O_2-induced death (ANOVA; $p < 0.0001$, $n = 3$). Data are represented as mean ± SEM. Right panels: Lysates of 293T cells transfected with FOXO3, FOXO3R, FOXO3R S207A, FOXO3R 4A, or their control vector were immunoblotted with the FOXO3 or ERK1/2 antibodies.

et al., 2004). We also tested whether knockdown induces pathological features of aging muscle in nematodes. As described for aging *C. elegans* (Herndon et al., 2002), sarcomeres of aging CST knockdown nematodes appeared more disorganized, containing discontinuities and bends in muscle fibers, when compared to control nematodes (Figure 6G and data not shown). CST knockdown also led to the premature appearance of age-associated oily droplets when compared to control N2 nematodes (Figure 6H) (Herndon et al., 2002). These results suggest that CST knockdown accelerates tissue aging together with reducing life span.

Importantly, overexpression of *cst-1* in *C. elegans* delayed the appearance of physical markers of aging as compared to control nematodes. Nematodes in which *cst-1* was overexpressed (*Ex1050*) demonstrated a delay in the development of age-associated oily droplets (Figure 6H) and were active for a longer period of time than control nematodes (Figure 6I). Together, our results suggest that CST-1 specifically promotes longevity and delays aging.

We next determined whether CST-1 promotes nematode life span in a DAF-16-dependent manner. We assessed the effect of *cst-1* overexpression on nematode life span in the background of *daf-16* RNAi. Induction

(F) Neurons transfected with GFP-FOXO3 or GFP-FOXO3 S207A were left untreated or treated with H_2O_2 for 1 hr and subjected to immunocytochemical analysis using confocal microscopy. H_2O_2 induced the nuclear translocation of GFP-FOXO3 but not GFP-FOXO3 S207A. Quantitation (average of two independent experiments) is shown.

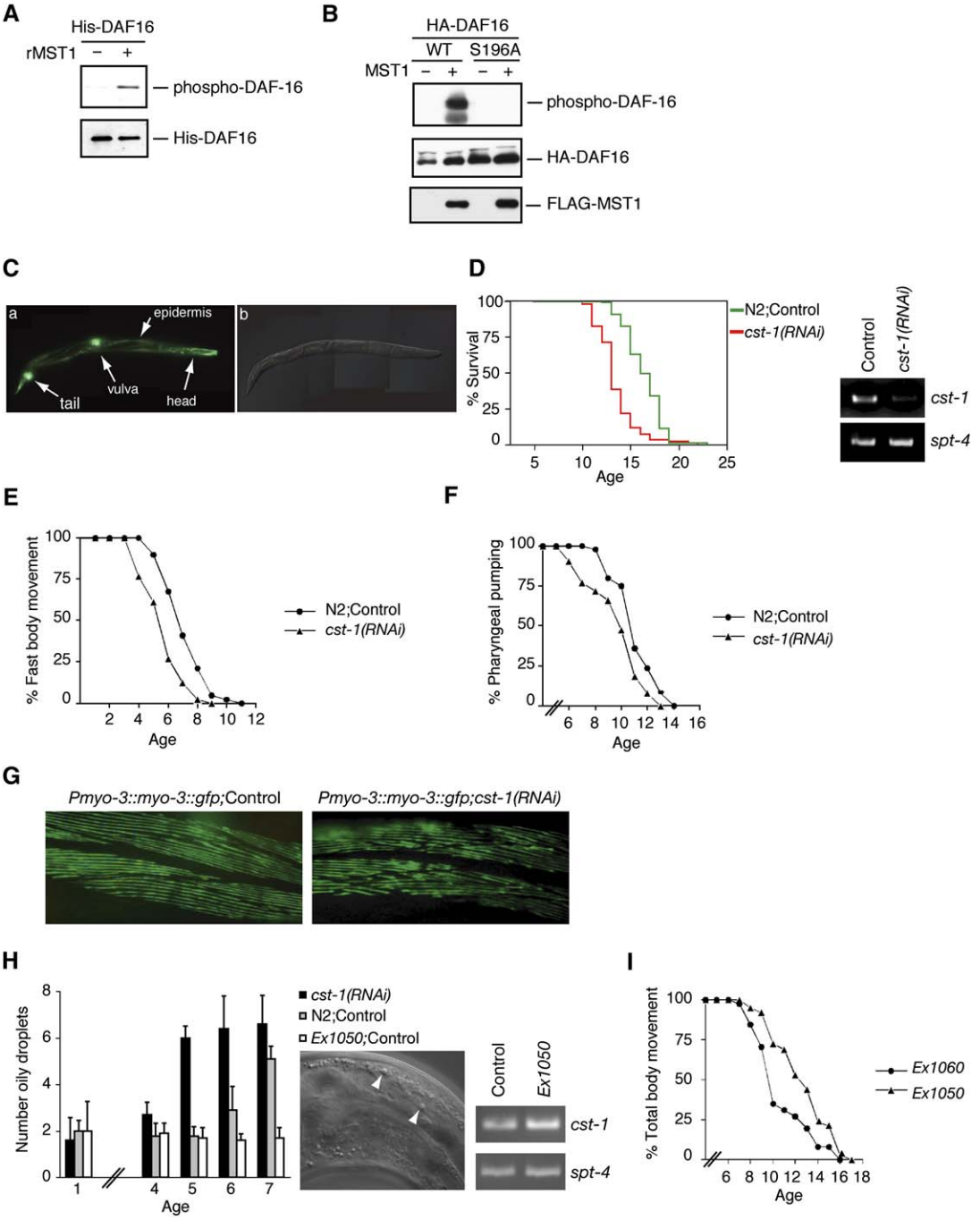

Figure 6. MST-FOXO Signaling Promotes Longevity in *C. elegans*

(A) In vitro kinase assays were carried out by incubating recombinant MST1 (Upstate) together with recombinant His-DAF-16 followed by immunoblotting with the phospho-FOXO or His antibody.

(B) Lysates of 293T cells transfected with an expression plasmid encoding HA-DAF-16 or HA-DAF-16 S196A together with the FLAG-MST1 expression vector or control plasmid were immunoblotted with the phospho-FOXO, HA, or FLAG antibody.

(Ca and Cb) *Pcst1::gfp* expression in wild-type nematodes. Fluorescent (Ca) and Nomarski (Cb) views of an L4 nematode are shown and are representative of more than five independent transgenic lines at all postembryonic stages examined (L1–adult; data not shown).

(D) Left panel: CST knockdown shortens nematode life span. For statistical analysis, see Table S2. Right panels: RT-PCR from synchronized L4 nematodes maintained on bacteria harboring the *cst-1* RNAi plasmid or control bacteria for two generations.

(E and F) CST knockdown reduced body movement when compared to control (log rank, $p < 0.0001$; animals observed/initial number examined: N2 = 42/53, *cst-1(RNAi)* = 42/50). CST knockdown also reduced pharyngeal pumping when compared to control (log rank, $p < 0.01$; animals observed/number examined: N2 = 39/53, *cst-1(RNAi)* = 38/50).

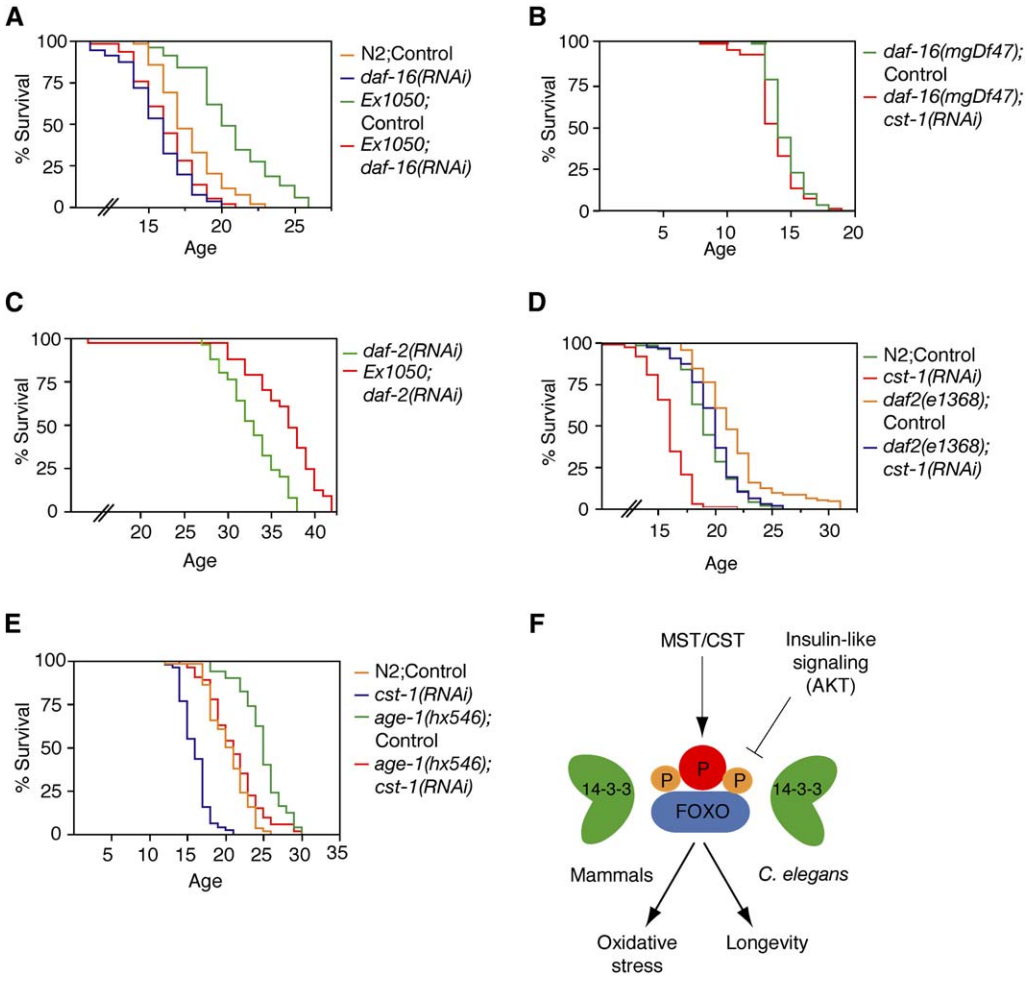

Figure 7. CST-1 Promotes Life Span in a DAF-16-Dependent Manner

(A) Life-span extension induced by overexpression of *cst-1* is *daf-16* dependent. *Ex1050* and N2 nematodes were fed bacteria containing the *daf-16* RNAi plasmid. For statistical analyses, see Table S2.

(B) CST knockdown does not influence life span of *daf-16(mgDf47)* nematodes.

(C) Overexpression of *cst-1* increases DAF-2 knockdown nematode life span.

(D and E) CST knockdown reduces life span in *daf-2(e1368)* and *age-1(hx546)* nematodes to an extent similar to in control N2 nematodes.

(F) Model of the MST-FOXO signaling pathway.

of DAF-16 knockdown shortened life span (Figure 7A and Table S2). While *cst-1* overexpression extended life span, *daf-16* RNAi completely suppressed the ability of CST-1 to extend life span (Figure 7A and Table S2). In other experiments, CST knockdown failed to reduce life span of DAF-16-deficient (*daf-16[mgDf47]*) nematodes (Figure 7B and Table S2). Taken together, these results suggest that DAF-16 acts downstream of CST-1 in life-span extension.

We also analyzed the relationship of CST-1 and the insulin signaling pathway in life-span control. Overexpression of *cst-1* increased life span of *daf-2* RNAi nematodes (Figure 7C and Table S2). In addition, CST knockdown reduced life span to a similar extent in both N2 and DAF-2-deficient *daf-2(e1368) C. elegans* as well as in both *age-1(hx546)* and N2 nematodes (Figures 7D and 7E and Table S2) (Gems et al., 1998; Friedman and Johnson,

(G) CST knockdown in *Pmyo-3::myo-3::gfp* nematodes promoted advanced muscle deterioration, including sarcomere disorganization, bending, and fragmentation. Images are representative of day 14 adult nematodes.

(H) Age-associated oily droplets between the pharyngeal bulbs developed earlier in response to CST knockdown when compared to control N2 nematodes (days 5 and 6; ANOVA; $p < 0.05$). Increased *cst-1* expression delayed the onset and progression of oily droplets (day 7; ANOVA; $p < 0.01$). Data are represented as mean ± SEM. Arrowheads in middle panel indicate representative oily droplets. Right panels: Increased *cst-1* gene dosage in *Ex1050* nematodes is shown by RT-PCR from young adult nematodes.

(I) *C. elegans* movement was scored by their ability to move during a 20 s time interval in response to gentle tapping of plates. Increased gene dosage of *cst-1* delays the onset of age-related physiological processes (log rank, $p < 0.01$; n: *Ex1060* = 26/50, *Ex1050* = 39/55).

1988). Since the *daf-2(e1368)* and *age-1(hx546)* alleles are non-null, epistasis between these genes and *cst-1* cannot be definitively determined. However, taken together, our findings support a model in which CST functions in parallel with the DAF-2 signaling pathway, converging on DAF-16 to regulate life span (see model in Figure 7F).

In summary, our genetic experiments in *C. elegans* strongly suggest that the MST-FOXO signaling pathway we uncovered in mammalian cells is conserved in nematodes. MST activates FOXO function in both mammalian cells and nematodes. Thus, while MST1-induced phosphorylation of FOXO3 activates FOXO3-dependent cell death in mammalian neurons in response to oxidative stress, the nematode MST1 ortholog CST-1 activates DAF-16 function and thus promotes life-span extension and delays aging of nematodes in a DAF-16-dependent manner.

DISCUSSION

In this study, we have discovered an evolutionarily conserved signaling link between the MST family of kinases and the FOXO transcription factors that mediates responses to oxidative stress in mammalian cells and promotes longevity in nematodes (Figure 7F). The identification of the FOXO proteins as major targets of MST suggests that these protein kinases play key roles in diverse biological processes including cellular homeostasis and longevity.

Our study implicates the MST family of kinases as a key mediator of cellular responses to oxidative stress in higher eukaryotes. Oxidative stress in mammalian cells induces the MST1-mediated phosphorylation of FOXO3 at serine 207, leading to the release of FOXO3 from 14-3-3 proteins and consequent accumulation of FOXO3 in the nucleus, where FOXO3 induces expression of cell death genes (Figure 7F). Activation of FOXO-dependent transcription can lead to either cell death or cell recovery in response to oxidative stress, depending on the severity of the stimulus (Brunet et al., 2004; Essers et al., 2004). The participation of FOXO proteins may thus serve to expand the range of MST-induced cellular responses accompanying oxidative stress to include adaptive responses.

A key conclusion of our study is that the MST-FOXO signaling link is conserved. The characterization of the *C. elegans* ortholog CST-1 broadens MST functions beyond the control of cell death to the regulation of life span. In nematodes, the FOXO protein DAF-16 does not appear to have functions in cell death and instead plays a central role in longevity (Kenyon, 2005). Thus, CST-1 activation of DAF-16 provides a positive signal for life-span extension. Since DAF-16 promotes life-span regulation via a complex array of changes in gene expression (Lee et al., 2003a; McElwee et al., 2004; Murphy et al., 2003), it will be important to identify the set of DAF-16 target genes that are regulated by CST-1. In our experiments, *cst-1* overexpression in nematodes induced the expression of the DAF-16 target gene *hsp-12.6* (Figure S6), which is thought to contribute to DAF-16-dependent life-span extension (Hsu et al., 2003).

An important goal of future studies is to determine how CST-DAF-16 signaling is regulated in *C. elegans*. Although we have found that the MST-FOXO pathway is activated by oxidative stress in mammalian cells, the nature of environmental conditions that regulate CST1's function in longevity remains to be identified. The relationship between oxidative stress and life-span control in *C. elegans* is unclear. Long-lived nematodes carrying mutations of components of the DAF-2 signaling pathway are resistant to stress signals including reactive oxygen species (Honda and Honda, 2002). Consistent with these results, antioxidant and other stress-response genes constitute a prominent set of DAF-16-regulated genes (Lee et al., 2003a; McElwee et al., 2004; Murphy et al., 2003). However, the role of antioxidant genes, including the widely studied gene superoxide dismutase *sod-3*, in life-span regulation in *C. elegans* remains to be established (Landis and Tower, 2005). Recent studies also point to several circumstances that uncouple life-span extension from resistance to stress signals (Lee et al., 2003b; Libina et al., 2003). In view of these observations, further studies of the CST-DAF-16 pathway may help shed light on the role of stress signals in longevity.

The elucidation of the MST1-induced phosphorylation of FOXO proteins and consequent disruption of their interaction with 14-3-3 proteins provides a molecular basis for how MST kinases activate FOXO signaling in both contexts of responses to oxidative stress in mammalian cells and the promotion of longevity in nematodes (Figure 7F). Growth factors induce the Akt-mediated phosphorylation of FOXOs at distinct sites stimulating interaction with 14-3-3 proteins, which in turn both promote the nuclear export and inhibit the nuclear import of FOXO proteins (reviewed in Van Der Heide et al., 2004). The MST1-induced phosphorylation of FOXO proteins disrupts their interaction with 14-3-3 proteins and consequently promotes the nuclear accumulation of FOXOs. These observations support a model in which MST/CST-induced phosphorylation of FOXO/DAF-16 opposes growth-factor regulation of FOXO transcription factors. Thus, the MST signal is a modulator of the insulin/IGF1-regulated PI3K-Akt-FOXO signaling pathway at the level of FOXO proteins.

Recent evidence suggests that the protein kinase JNK also signals via FOXO proteins to trigger cellular and organism-wide responses by opposing growth-factor regulation of FOXO proteins (Essers et al., 2004; Oh et al., 2005; Wang et al., 2005). JNK phosphorylates FOXO4 within the transactivation domain (Essers et al., 2004). In our experiments, JNK failed to phosphorylate the forkhead domain of FOXO proteins in vitro (data not shown), suggesting that MST1 phosphorylates the conserved FOXO forkhead-domain site independently of JNK. Together, these observations raise the possibility that MST1 and JNK may cooperate in the activation of FOXO proteins, whereby MST1 triggers the translocation of

FOXOs to the nucleus to set the stage for JNK-induced phosphorylation of the FOXO transactivation domain.

In this study, we focused on the role of the MST-FOXO signaling pathway in responses to oxidative stress in mammalian cells and life-span control in nematodes. However, identification of the signaling link between the MST kinases and the FOXO transcription factors points to new biological roles for both families of proteins. It will be interesting to consider the potential role of FOXO proteins downstream of MST kinases in cell death induced by other stimuli in addition to oxidative stress, including the activation of tumor suppressors (Khokhlatchev et al., 2002). Since the FOXO transcription factors influence cell metabolism, differentiation, and transformation (Accili and Arden, 2004), our findings also raise the possibility that MST might play important roles in these fundamental biological processes. In a similar vein, the role of FOXOs in pathological states including cancer and diabetes mellitus (Hu et al., 2004; Nakae et al., 2002) points to the possibility that misregulation of MST-FOXO signaling might contribute to the pathogenesis of these disorders. Finally, elucidation of the MST-FOXO signaling pathway as a key mediator of oxidative-stress-induced neuronal cell death raises the important question of whether activation of this signaling pathway might contribute to the pathogenesis of neurologic diseases.

EXPERIMENTAL PROCEDURES

Plasmids

Fragments of GST-FOXO3 and GST-FOXO1 forkhead-domain plasmids were cloned by PCR into pGEX4T1 at the EcoRI and XhoI restriction sites. His-FOXO3 was cloned into pET3a vector at the EcoRI and BamHI restriction sites. FOXO3 S207A and 4A and FOXO1 S212A and 4A were generated by site-directed mutagenesis. All mutations were verified by sequencing.

Antibodies

Antibodies to MST1 (Zymed); phospho-MST1(Thr183)/MST2(Thr180), MST2, and ERK1/2 (Cell Signaling); FOXO3 (Upstate); GFP (Molecular Probes); GST, MLK3, His, HA, 14-3-3β, Hsp60, and β-actin (Santa Cruz Biotechnology); FLAG-M2 (Sigma); and BIM (Stressgen) were purchased. The rabbit antibody to phosphorylated serine 207 of FOXO3 was generated by injecting New Zealand rabbits with the phosphopeptide antigen C-SAGWKNpSIRHNLS and was purified as described (Konishi et al., 2002).

Tissue Culture

Cerebellar granule neuron cultures were prepared from postnatal day 6 (P6) rat pups as described (Konishi et al., 2002). For RNAi experiments, cultures from P6 + 2 days in vitro (DIV) were transfected with the RNAi or control U6 plasmid together with a plasmid encoding β-galactosidase. After 3 days, cultures were left untreated or were treated with H_2O_2 (60–100 μM; Fisher) for 24 hr, fixed, and subjected to cell survival as described (Konishi et al., 2002). Cell counts were carried out in a blinded manner and analyzed for statistical significance by ANOVA followed by Fisher's PLSD post hoc test. Approximately 150 cells were counted per experiment. Unless stated otherwise, all transfections were done by a calcium-phosphate method as described (Konishi et al., 2002).

Immunoprecipitation, Immunoblotting, and Kinase Assays

In vitro kinase assays were carried out as described (Graves et al., 2001). Immunoprecipitations and immunoblotting were carried out as described (Konishi et al., 2002).

Mass Spectrometry

Coomassie blue-stained bands corresponding to FOXO3 and FOXO1 (unphosphorylated or phosphorylated with MST1) were digested with trypsin as described (Peng and Gygi, 2001). Peptide mixtures were separated by reverse-phase chromatography and online analyzed on a hybrid linear ion trap/ion cyclotron resonance Fourier transform instrument (LTQ-FT, Thermo Finnigan) using a TOP10 method. MS3 scans were triggered only for doubly charged ions demonstrating an intense neutral loss of phosphoric acid (Beausoleil et al., 2004). Spectra were searched using the SEQUEST algorithm. Peptide matches obtained were deemed correct after applying several filtering criteria (tryptic ends, XCorr > 1.8 and 2.7 for 2+ and 3+ ions, respectively; mass error < 5 ppm) and manual validation.

RNAi Plasmid Design

Mammalian RNAi constructs were designed as described (Gaudilliere et al., 2002). The hpRNA targeting sequences used include MST1 hpRNA: GGGCACTGTCCGAGTAGCAGC; MST2 hpRNA: GCAATACTGTAATAGGAACTC; and FOXO hpRNA: GAGCGTGCCCTACTTCAAGGA. MST1 Rescue and FOXO Rescue were generated by creating five silent base-pair mutations into the wild-type cDNA encoding MST1 or FOXO3 using the QuikChange Site-Directed Mutagenesis Kit (Stratagene). For *cst-1* RNAi experiments, a cDNA fragment of *cst-1* (nucleotides 121–1141) was generated by PCR from cDNA clone yk103e9.

Extrachromosomal Transgenic *C. elegans*

To examine the expression pattern of *cst-1*, ~1.7 kb of the predicted promoter region was cloned into the GFP expression vector pPD95.75 (*Pcst1::gfp*). The *Pcst1::gfp* plasmid (50 ng/μl) was injected together with the pRF4 (*rol-6(su1006)*) plasmid (100 ng/μl), which was used as the transformation marker in all experiments. To express CST-1, the endogenous locus including ~1.7 kb of upstream regulatory sequence and the entire coding and 3′UTR regions was cloned into pBs (pBs-*cst-1*) and injected at 2.5 ng/μl.

C. elegans Life-Span Analysis

Life-span experiments were carried out as described (An and Blackwell, 2003). Each experiment was carried out over several plates such that for an experiment with n = 100, four plates containing 25 nematodes were used. During life-span analysis, *C. elegans* were observed daily for movements. If no movement was detected, nematodes were prodded gently with a platinum wire and examined for pharyngeal pumping to determine whether alive. Worms that escaped from the plates or exploded were censored. Statistical analysis (log rank, Mantel-Cox) was carried out using JMP-IN 5.1 statistical software. Maximal life span of *Ex1050* and N2 nematodes in each experiment was calculated by obtaining the mean ± SEM of maximum life span of all plates in each experiment and was subjected to statistical analysis using the t test.

Supplemental Data

Supplemental Data include Supplemental Experimental Procedures, six figures, and two tables and can be found with this article online at http://www.cell.com/cgi/content/full/125/5/987/DC1/.

ACKNOWLEDGMENTS

We thank J. Blenis, G. Corfas, A. Hart, and L.-H. Tsai for helpful discussions; members of the Bonni laboratory for critical reading of the manuscript and helpful discussions; Z. Zheng for statistical advice; M. Smidt for providing GFP-FOXO3; J. Avruch for MST plasmids; J. Chernoff for MST1 antibodies; J. Ham for pGL3-BIM; Y. Shi for

His-DAF-16; A. Fire for pPD95.75; G. Ruvkun for the *daf-2* and *daf-16* RNAi constructs; and W. Mohler for *Pmyo-3::myo-3::gfp* nematodes. This work was supported by NIH grants NS41021 (A.B.) and GM62891 (T.K.B.) and fellowships from the NSF (M.K.L. and Y.Y.), Glenn/AFAR (M.K.L.), the Albert J. Ryan Foundation (M.K.L. and E.B.E.B.), the Lefler Foundation (Z.Y.), and the Myra Reinhard Family Foundation (P.R.B.). A.B. is the recipient of a fellowship from the Alfred P. Sloan Foundation, a Robert H. Ebert Clinical Scholar Award from the Esther A. and Joseph Klingenstein Fund, an EJLB Foundation award, and a Sidney Kimmel Foundation Award. We apologize to authors whose work was not cited owing to space limitations.

Received: July 28, 2005
Revised: January 16, 2006
Accepted: March 31, 2006
Published: June 1, 2006

REFERENCES

Accili, D., and Arden, K.C. (2004). FoxOs at the crossroads of cellular metabolism, differentiation, and transformation. Cell *117*, 421–426.

Ahn, S.H., Cheung, W.L., Hsu, J.Y., Diaz, R.L., Smith, M.M., and Allis, C.D. (2005). Sterile 20 kinase phosphorylates histone H2B at serine 10 during hydrogen peroxide-induced apoptosis in S. cerevisiae. Cell *120*, 25–36.

An, J.H., and Blackwell, T.K. (2003). SKN-1 links C. elegans mesendodermal specification to a conserved oxidative stress response. Genes Dev. *17*, 1882–1893.

Beausoleil, S.A., Jedrychowski, M., Schwartz, D., Elias, J.E., Villen, J., Li, J., Cohn, M.A., Cantley, L.C., and Gygi, S.P. (2004). Large-scale characterization of HeLa cell nuclear phosphoproteins. Proc. Natl. Acad. Sci. USA *101*, 12130–12135.

Becker, E.B., and Bonni, A. (2004). Cell cycle regulation of neuronal apoptosis in development and disease. Prog. Neurobiol. *72*, 1–25.

Beckman, K.B., and Ames, B.N. (1998). The free radical theory of aging matures. Physiol. Rev. *78*, 547–581.

Brunet, A., Datta, S.R., and Greenberg, M.E. (2001). Transcription-dependent and -independent control of neuronal survival by the PI3K-Akt signaling pathway. Curr. Opin. Neurobiol. *11*, 297–305.

Brunet, A., Sweeney, L.B., Sturgill, J.F., Chua, K.F., Greer, P.L., Lin, Y., Tran, H., Ross, S.E., Mostoslavsky, R., Cohen, H.Y., et al. (2004). Stress-dependent regulation of FOXO transcription factors by the SIRT1 deacetylase. Science *303*, 2011–2015.

Burgering, B.M., and Kops, G.J. (2002). Cell cycle and death control: long live Forkheads. Trends Biochem. Sci. *27*, 352–360.

Cheung, W.L., Ajiro, K., Samejima, K., Kloc, M., Cheung, P., Mizzen, C.A., Beeser, A., Etkin, L.D., Chernoff, J., Earnshaw, W.C., and Allis, C.D. (2003). Apoptotic phosphorylation of histone H2B is mediated by mammalian sterile twenty kinase. Cell *113*, 507–517.

Chong, Z.Z., Li, F., and Maiese, K. (2005). Oxidative stress in the brain: novel cellular targets that govern survival during neurodegenerative disease. Prog. Neurobiol. *75*, 207–246.

Essers, M.A., Weijzen, S., de Vries-Smits, A.M., Saarloos, I., de Ruiter, N.D., Bos, J.L., and Burgering, B.M. (2004). FOXO transcription factor activation by oxidative stress mediated by the small GTPase Ral and JNK. EMBO J. *23*, 4802–4812.

Finkel, T. (2000). Redox-dependent signal transduction. FEBS Lett. *476*, 52–54.

Friedman, D.B., and Johnson, T.E. (1988). A mutation in the age-1 gene in Caenorhabditis elegans lengthens life and reduces hermaphrodite fertility. Genetics *118*, 75–86.

Gaudilliere, B., Shi, Y., and Bonni, A. (2002). RNA interference reveals a requirement for myocyte enhancer factor 2A in activity-dependent neuronal survival. J. Biol. Chem. *277*, 46442–46446.

Gems, D., Sutton, A.J., Sundermeyer, M.L., Albert, P.S., King, K.V., Edgley, M.L., Larsen, P.L., and Riddle, D.L. (1998). Two pleiotropic classes of daf-2 mutation affect larval arrest, adult behavior, reproduction and longevity in Caenorhabditis elegans. Genetics *150*, 129–155.

Giannakou, M.E., Goss, M., Junger, M.A., Hafen, E., Leevers, S.J., and Partridge, L. (2004). Long-lived Drosophila with overexpressed dFOXO in adult fat body. Science *305*, 361.

Gilley, J., Coffer, P.J., and Ham, J. (2003). FOXO transcription factors directly activate bim gene expression and promote apoptosis in sympathetic neurons. J. Cell Biol. *162*, 613–622.

Graves, J.D., Gotoh, Y., Draves, K.E., Ambrose, D., Han, D.K., Wright, M., Chernoff, J., Clark, E.A., and Krebs, E.G. (1998). Caspase-mediated activation and induction of apoptosis by the mammalian Ste20-like kinase Mst1. EMBO J. *17*, 2224–2234.

Graves, J.D., Draves, K.E., Gotoh, Y., Krebs, E.G., and Clark, E.A. (2001). Both phosphorylation and caspase-mediated cleavage contribute to regulation of the Ste20-like protein kinase Mst1 during CD95/Fas-induced apoptosis. J. Biol. Chem. *276*, 14909–14915.

Harvey, K.F., Pfleger, C.M., and Hariharan, I.K. (2003). The Drosophila Mst ortholog, hippo, restricts growth and cell proliferation and promotes apoptosis. Cell *114*, 457–467.

Herndon, L.A., Schmeissner, P.J., Dudaronek, J.M., Brown, P.A., Listner, K.M., Sakano, Y., Paupard, M.C., Hall, D.H., and Driscoll, M. (2002). Stochastic and genetic factors influence tissue-specific decline in ageing C. elegans. Nature *419*, 808–814.

Honda, Y., and Honda, S. (2002). Oxidative stress and life span determination in the nematode Caenorhabditis elegans. Ann. N Y Acad. Sci. *959*, 466–474.

Hsu, A.L., Murphy, C.T., and Kenyon, C. (2003). Regulation of aging and age-related disease by DAF-16 and heat-shock factor. Science *300*, 1142–1145.

Hu, M.C., Lee, D.F., Xia, W., Golfman, L.S., Ou-Yang, F., Yang, J.Y., Zou, Y., Bao, S., Hanada, N., Saso, H., et al. (2004). IkappaB kinase promotes tumorigenesis through inhibition of forkhead FOXO3a. Cell *117*, 225–237.

Huang, C., Xiong, C., and Kornfeld, K. (2004). Measurements of age-related changes of physiological processes that predict lifespan of Caenorhabditis elegans. Proc. Natl. Acad. Sci. USA *101*, 8084–8089.

Hwangbo, D.S., Gershman, B., Tu, M.P., Palmer, M., and Tatar, M. (2004). Drosophila dFOXO controls lifespan and regulates insulin signalling in brain and fat body. Nature *429*, 562–566.

Karin, M., and Hunter, T. (1995). Transcriptional control by protein phosphorylation: signal transmission from the cell surface to the nucleus. Curr. Biol. *5*, 747–757.

Kenyon, C. (2005). The plasticity of aging: insights from long-lived mutants. Cell *120*, 449–460.

Khokhlatchev, A., Rabizadeh, S., Xavier, R., Nedwidek, M., Chen, T., Zhang, X.F., Seed, B., and Avruch, J. (2002). Identification of a novel Ras-regulated proapoptotic pathway. Curr. Biol. *12*, 253–265.

Konishi, Y., Lehtinen, M., Donovan, N., and Bonni, A. (2002). Cdc2 phosphorylation of BAD links the cell cycle to the cell death machinery. Mol. Cell *9*, 1005–1016.

Kops, G.J., Dansen, T.B., Polderman, P.E., Saarloos, I., Wirtz, K.W., Coffer, P.J., Huang, T.T., Bos, J.L., Medema, R.H., and Burgering, B.M. (2002). Forkhead transcription factor FOXO3a protects quiescent cells from oxidative stress. Nature *419*, 316–321.

Landis, G.N., and Tower, J. (2005). Superoxide dismutase evolution and life span regulation. Mech. Ageing Dev. *126*, 365–379.

Lee, S.S., Kennedy, S., Tolonen, A.C., and Ruvkun, G. (2003a). DAF-16 target genes that control C. elegans life-span and metabolism. Science *300*, 644–647.

Lee, S.S., Lee, R.Y., Fraser, A.G., Kamath, R.S., Ahringer, J., and Ruvkun, G. (2003b). A systematic RNAi screen identifies a critical role for mitochondria in C. elegans longevity. Nat. Genet. *33*, 40–48.

Libina, N., Berman, J.R., and Kenyon, C. (2003). Tissue-specific activities of C. elegans DAF-16 in the regulation of lifespan. Cell *115*, 489–502.

McElwee, J.J., Schuster, E., Blanc, E., Thomas, J.H., and Gems, D. (2004). Shared transcriptional signature in Caenorhabditis elegans Dauer larvae and long-lived daf-2 mutants implicates detoxification system in longevity assurance. J. Biol. Chem. *279*, 44533–44543.

Murphy, C.T., McCarroll, S.A., Bargmann, C.I., Fraser, A., Kamath, R.S., Ahringer, J., Li, H., and Kenyon, C. (2003). Genes that act downstream of DAF-16 to influence the lifespan of Caenorhabditis elegans. Nature *424*, 277–283.

Nakae, J., Biggs, W.H., 3rd, Kitamura, T., Cavenee, W.K., Wright, C.V., Arden, K.C., and Accili, D. (2002). Regulation of insulin action and pancreatic beta-cell function by mutated alleles of the gene encoding forkhead transcription factor Foxo1. Nat. Genet. *32*, 245–253.

Oh, S.W., Mukhopadhyay, A., Svrzikapa, N., Jiang, F., Davis, R.J., and Tissenbaum, H.A. (2005). JNK regulates lifespan in Caenorhabditis elegans by modulating nuclear translocation of forkhead transcription factor/DAF-16. Proc. Natl. Acad. Sci. USA *102*, 4494–4499.

O'Neill, E., Rushworth, L., Baccarini, M., and Kolch, W. (2004). Role of the kinase MST2 in suppression of apoptosis by the proto-oncogene product Raf-1. Science *306*, 2267–2270.

Peng, J., and Gygi, S.P. (2001). Proteomics: the move to mixtures. J. Mass Spectrom. *36*, 1083–1091.

Van Der Heide, L.P., Hoekman, M.F., and Smidt, M.P. (2004). The ins and outs of FoxO shuttling: mechanisms of FoxO translocation and transcriptional regulation. Biochem. J. *380*, 297–309.

Wang, M.C., Bohmann, D., and Jasper, H. (2005). JNK extends life span and limits growth by antagonizing cellular and organism-wide responses to insulin signaling. Cell *121*, 115–125.

Wu, S., Huang, J., Dong, J., and Pan, D. (2003). hippo encodes a Ste-20 family protein kinase that restricts cell proliferation and promotes apoptosis in conjunction with salvador and warts. Cell *114*, 445–456.